Microwave Journal
Frequency Matters.

www.microwavejournal.com/articles/35761-the-impact-of-stray-magnetic-fields-on-the-performance-of-faraday-rotation-isolators

Online Spotlight: The Impact of Stray Magnetic Fields on the Performance of Faraday Rotation Isolators

David W. Porterfield, Jr, Ph.D., Micro Harmonics Corporation
April 6, 2021

Traditional style isolators sold commercially over the past 50 years are highly susceptible to low level stray magnetic fields. Even in relatively weak stray fields, insertion loss can exceed 30 dB rendering the device unusable. In contrast, newer magnetically saturated type isolators function remarkably well in stray fields.

Faraday rotation isolators employ magnetically biased ferrite rods to rotate the polarization of an RF signal and are thus susceptible to stray magnetic fields. Stray magnetic fields are defined as those arising from sources external to the isolator and are not magnetic fields generated by the internal magnets used to bias the ferrite. The offending stray fields can arise from other nearby ferrite components but are also common in a variety of mmWave experiments like dynamic nuclear polarization,[1] particle accelerators[2] and tokamak fusion reactors.[3] Stray magnetic fields can, in principle, alter the magnetic bias point in the ferrite and cause under- or over-rotation of the RF signal resulting in increased insertion loss and decreased isolation. Test results described demonstrate that traditional style isolators sold commercially over the past 50 years are highly susceptible to low level stray magnetic fields. Even in relatively weak stray fields, insertion loss can exceed 30 dB rendering the device unusable. In contrast, newer magnetically saturated type isolators function remarkably well in stray fields up to and exceeding 250 Oe.

ISOLATOR OPERATION

Isolators are non-reciprocal devices, passing EM signals in one direction and absorbing them in the reverse direction. They are primarily used to suppress standing waves that arise from signal reflections caused by impedance mismatches between highly tuned components in microwave and mmWave systems. Standing waves limit system bandwidth and cause dips or even nulls in the final output. Standing waves can be mitigated by inserting isolators between mismatched components resulting in a smoother frequency response and improved bandwidth.

The isolator topology most frequently used at mmWave frequencies is the Faraday rotation type first described by Barnes in 1961.[4] This isolator employs a ceramic cone to couple a TE_{10} rectangular waveguide mode to a TE_{11} mode in a cylindrical ferrite rod. The signal polarization is rotated by 45 degrees as it passes through the ferrite rod and is then coupled to an output waveguide via a second ceramic cone.

Figure 1 shows the layout of the waveguides, ceramic cones and ferrite rod in a typical isolator. The black arrows at the center of the input and output waveguides indicate the polarization of the primary TE_{10} waveguide

mode. The input and output waveguides are canted at 45 degrees with respect to each other. The ferrite rod spans the gap between the waveguides and has a diameter roughly equal to the waveguide height. Each cone has a resistive layer that bisects the central axis. The resistive layers are oriented such that they are normal to the TE_{10} mode polarization in their respective waveguides.

Figure 2 shows the electric field polarization vector orientations of the forward and reverse traveling signals. Both signals rotate in the same direction (CCW for the purpose of this illustration). The forward traveling signal is normal to the resistive layers in both cones, minimizing loss and signal attenuation. The polarization vector of the reverse traveling signal is aligned with the resistive layer in the input waveguide causing the signal to be absorbed.

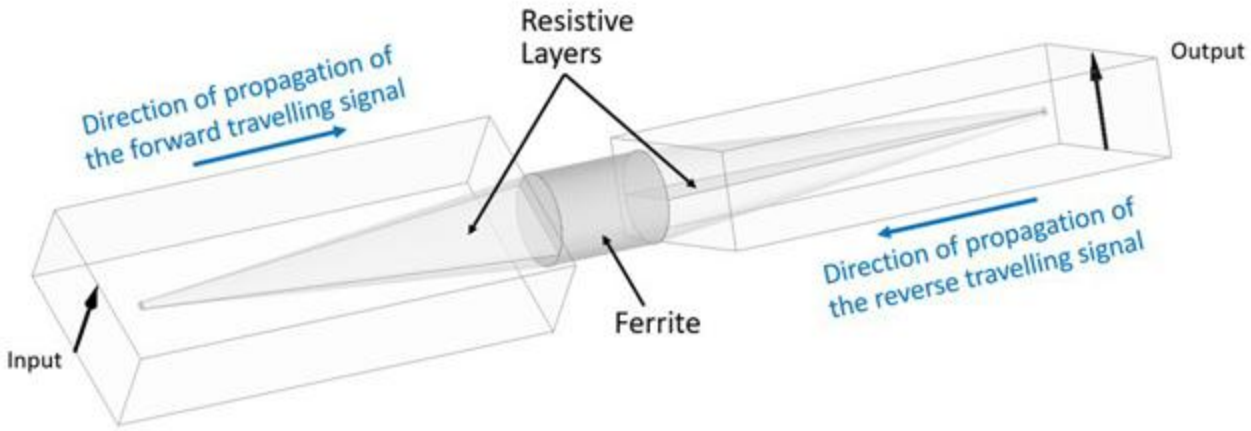

Figure 1 Sketch showing the waveguides, ceramic cones and ferrite rod in a Faraday rotation isolator.

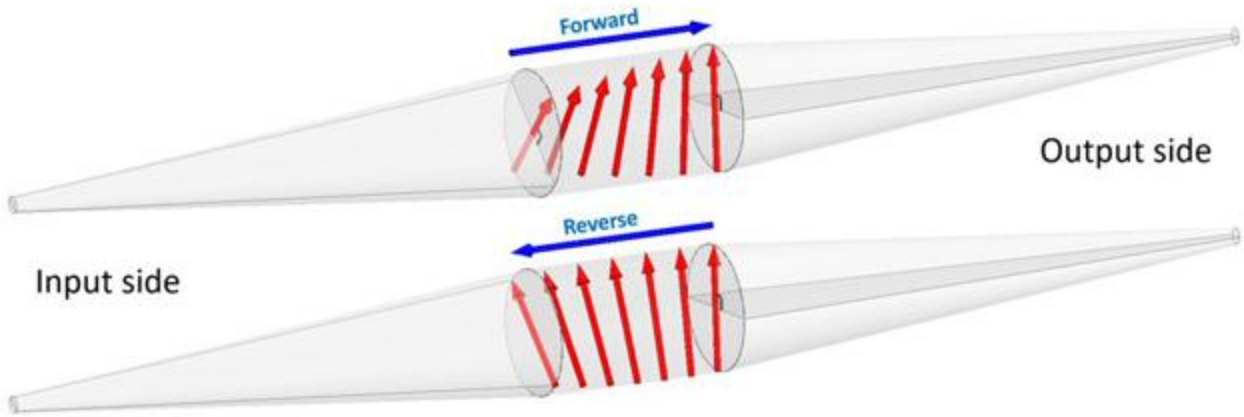

Figure 2 Rotation of the forward and reverse traveling signals as they pass through the ferrite rod.

The rotation angle, θ, of the signal as it passes through the ferrite rod is directly proportional to the ferrite magnetization, $4\pi M_Z$, and the ferrite length, l, as shown in Equation (1).

$$\theta = \frac{4\pi M_Z \Upsilon l \sqrt{\varepsilon}}{2c}$$

where, $4\pi M_Z$ is the axial magnetization

Υ is the gyromagnetic ratio,[5]

$$\gamma = g \times 8.795 \times 10^6 \ \frac{rad}{(s \cdot Oe)}, g = 2.11$$

l is the ferrite length

c is the speed of light

ε is the ferrite dielectric constant

An external magnetic field is used to align magnetic dipoles in the ferrite giving rise to the desired axial magnetization, $4\pi M_Z$. Rare earth magnets are often used, typically neodymium ($Nd_2Fe_{14}B$) or samarium cobalt ($SmCo_5$ or Sm_2Co_{17}). As the magnetic bias field increases, additional dipoles are aligned and the magnetization, $4\pi M_Z$, increases until reaching a point of saturation denoted as the saturation magnetization, $4\pi M_S$, beyond which further increases in the applied magnetic field have little effect. The magnitude of the saturation magnetization is a material dependent property and varies in the range 300-5000 gauss for most commercial ferrites. Ferrite material with $4\pi M_S$ = 5,000 gauss[5] is typically used in mmWave isolators. The saturation magnetization is temperature dependent, following a modified Bloch law and reaching a maximum value at absolute zero (0 K) since it is easier to align magnetic dipoles at lower kinetic energy levels.

The dipoles precess around the magnetic bias field vector as shown in **Figure 3**. As an EM signal passes through the ferrite, the fields interact with the dipole moments. Linearly polarized waves, like those passing through the isolator, can be decomposed into left-hand circularly polarized (LHCP) and right-hand circularly polarized (RHCP) waves. The interaction with the precessing dipole moments yields disparate propagation constants for the RHCP and LHCP waves. The difference in the propagation constants arises because one of the components (RHCP or LHCP) opposes the dipole precession and the other coincides with it. As a result, a phase shift occurs between the RHCP and LHCP waves as they propagate through the ferrite. This gives rise to the rotation of the linearly polarized signal. More in-depth discussions on Faraday rotation are given by Pozar,[6] Lax et al.[7] and Balanis.[8]

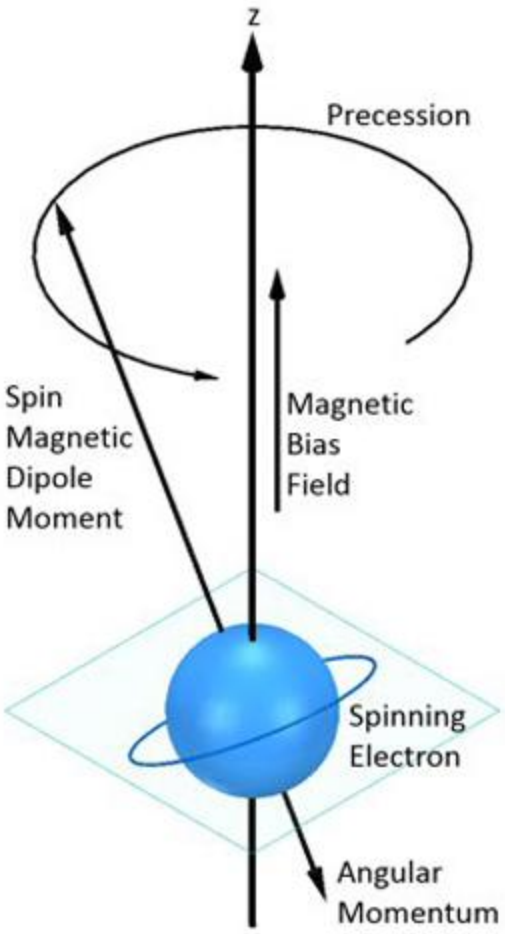

Figure 3 Angular momentum and spin magnetic dipole moment vectors.

Faraday rotation isolators can be classified into two basic categories: 1) magnetically saturated and 2) non-saturated (see **Figure 4**). They can usually, but not always, be identified by size and shape. A saturated isolator is smaller and does not have a magnetic sheath. The traditional non-saturated isolator is typically much larger and most have hollow cylindrical magnetic sheaths around their center sections.

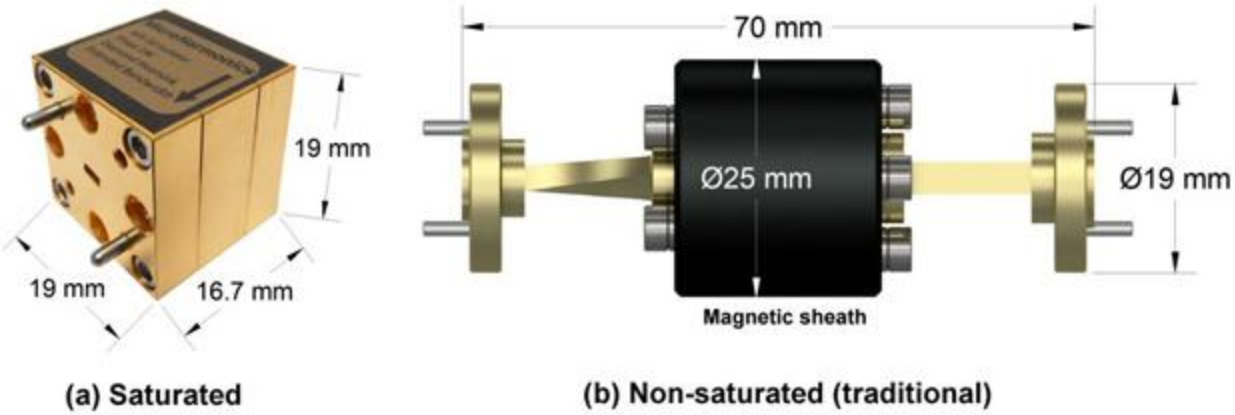

Figure 4 Saturated (a) and traditional non-saturated (b) WR-10 Faraday rotation isolators.

Figure 5 shows a traditional non-saturated Faraday rotation isolator with the magnetic sheath and waveguides removed. The magnetic bias field is adjusted by rotating the magnet off axis until maximum isolation is achieved and then locking down the magnet with an epoxy. The long ferrite rod used in the non-saturating isolators is lossy at mmWave frequencies leading to high insertion loss, but the ability to fine tune the rotation while testing in-situ is a powerful tool.

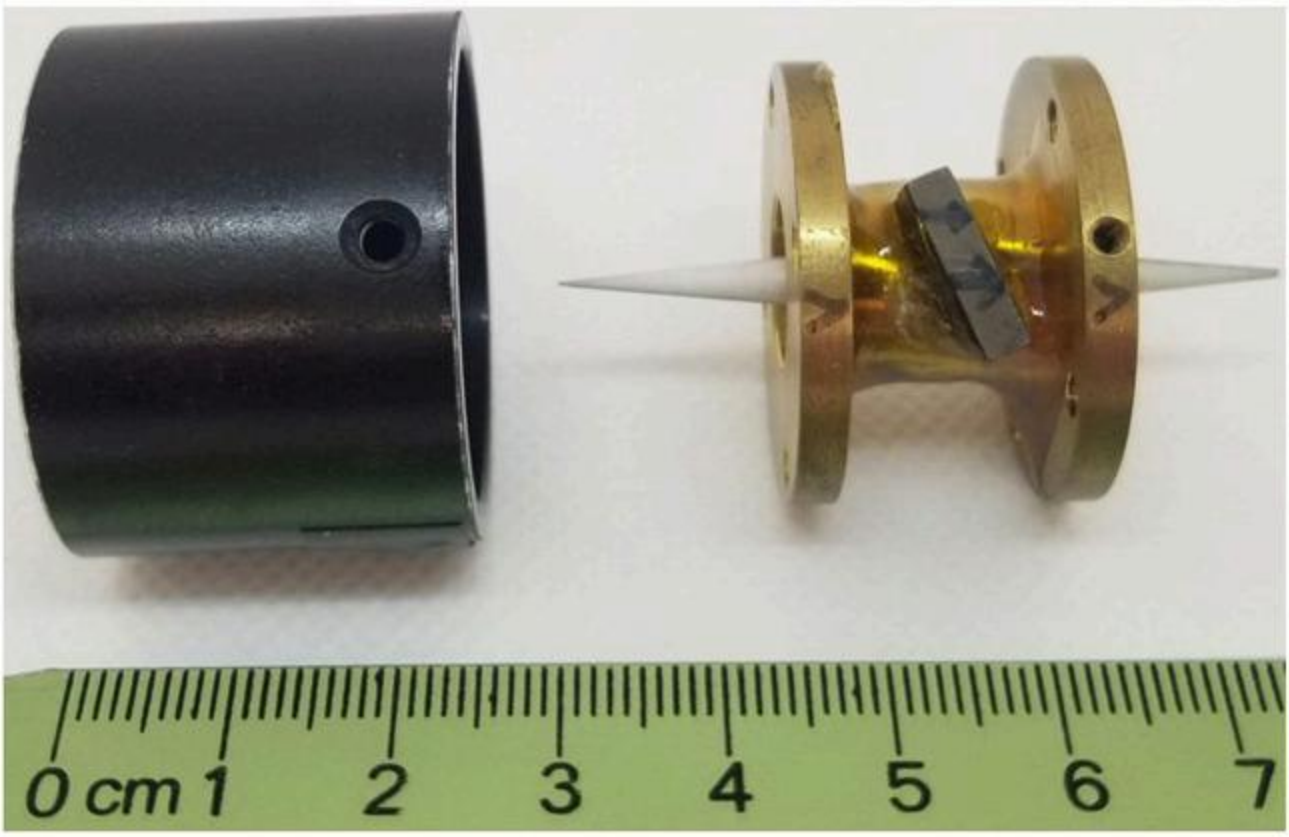

Figure 5 Canted magnet in a traditional isolator.

A saturated isolator use a much shorter ferrite rod and a saturating magnetic bias field to achieve the required 45 degrees of rotation. It is thus much smaller than the traditional isolator and has much lower insertion loss.

STRAY MAGNETIC FIELD TESTS

Laboratory tests are conducted in W-Band (75-110 GHz) to determine the effects of stray magnetic fields. Two isolators are tested, one made by Micro Harmonics (saturated type) and a traditional style isolator made by another vendor (unsaturated type). Since traditional style isolators have similar construction regardless of the manufacturer, the tested traditional style isolator is thought to be representative of its entire class. The tests are conducted using a Keysight N5222B PNA (vector network analyzer) and a pair of VDI W-Band frequency extenders. The isolators are subjected to both normal and axial stray magnetic fields. Normal stray fields are oriented at a 90 angle angle to the magnetic bias field and axial stray fields are parallel to the bias field. The test apparatus used to produce normal stray magnetic fields is shown in **Figure 6**. The maximum field produced by the apparatus is measured to be ± 65 Oe.

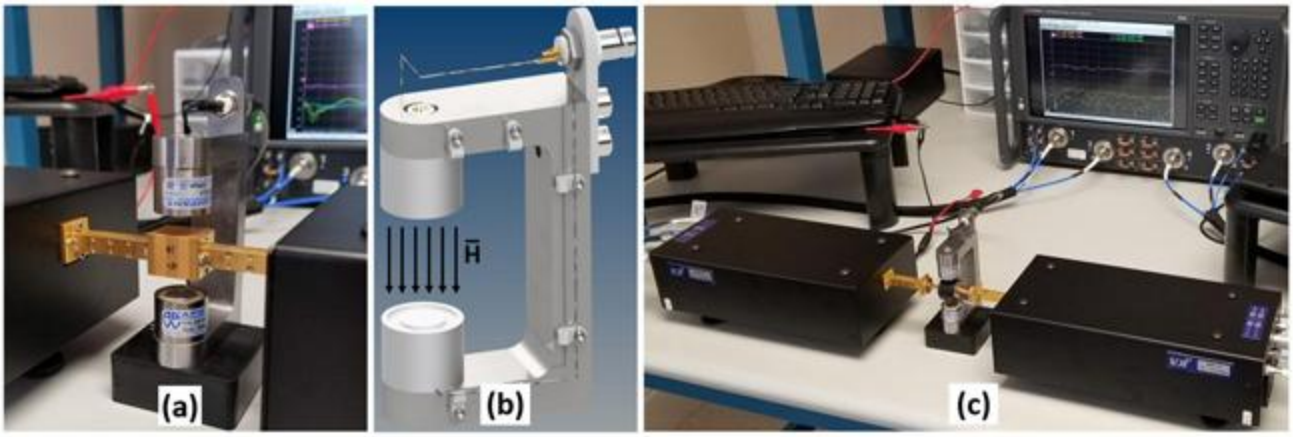

Figure 6 Saturated isolator in the normal stray field test fixture (a), sketch of normal stray field test apparatus showing the direction of the magnetic field (b) and a traditional style non-saturated isolator in the normal stray field test fixture (c).

A magnetic coil is used to produce the axial stray magnetic fields as shown in **Figure 7**. The coil has 787 turns of 24 AWG magnet wire, an inner diameter of 38 mm and a length of 25 mm. The maximum axial field is measured at more than ± 260 Oe at the coil center. Both normal and axial stray fields are calibrated using Hall effect sensors; however, magnetic materials used in the isolators may perturb the stray field intensity at the ferrite location when the isolators are inserted into the test apparatus.

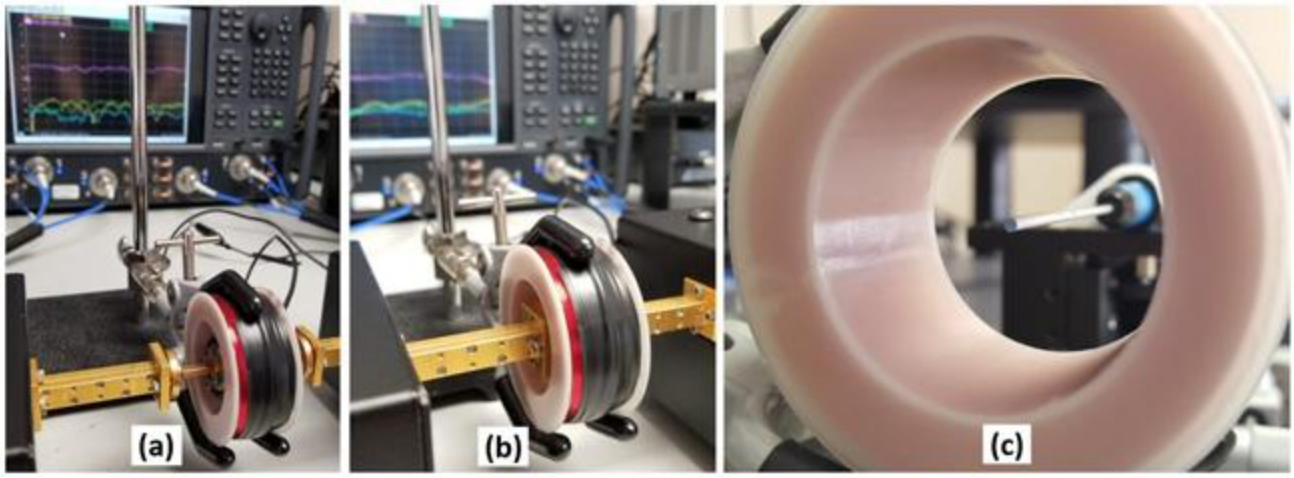

Figure 7 Traditional style isolator in the axial stray field test fixture (a), saturated isolator in the axial stray field test fixture (b) and the Hall probe calibration of the axial magnetic field coil (c).

Normal (Orthogonal) Stray Magnetic Field Tests

Full two port S-parameter data is recorded from 75 to 110 GHz as the calibrated normal stray magnetic field is varied. For simplicity, only data at the band center (92.5 GHz) is shown. Insertion loss (IL) and isolation (Iso) for the two isolators is shown in **Figure 8** for a normal stray magnetic field ranging from 0 to 65 Oe. Insertion loss of the saturated isolator remains nearly constant at 0.5 dB, while insertion loss of the traditional isolator remains constant at 1.7 dB. There is no change in isolation of the saturated isolator, which remains constant at 28 dB. Isolation of the traditional style unsaturated isolator, however, drops from 39 to 29 dB, a relatively minor effect.

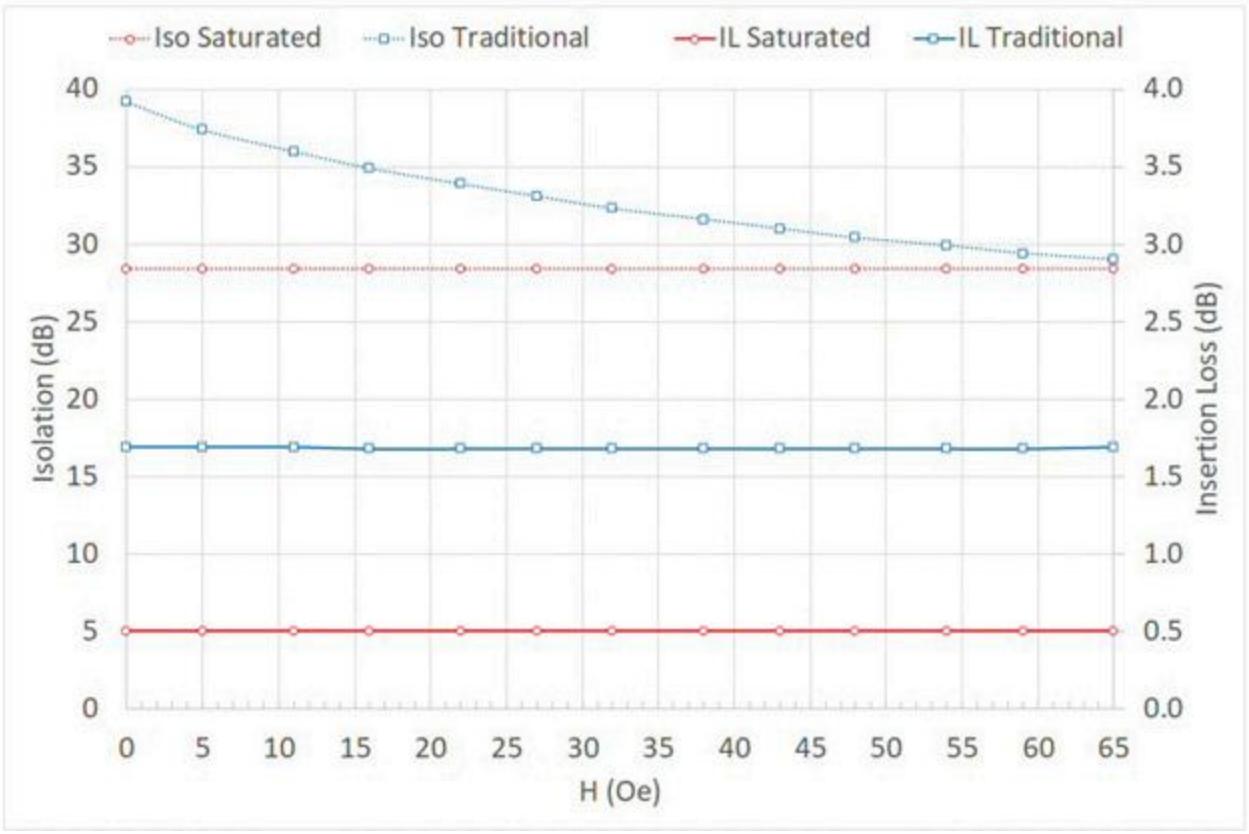

Figure 8 Test data for a saturated (red) and traditional style unsaturated isolator (blue) under a normal (orthogonal) stray magnetic field. The test data is taken at a W-Band center frequency of 92.5 GHz.

Both isolators perform well under exposure to orthogonal stray magnetic fields. The magnetic sheath used in the traditional isolator efficiently diverts the normal stray magnetic field around the isolator body and away from the ferrite. The strong magnetic bias field used in the saturated isolator keeps the magnetic dipoles aligned in the presence of the normal stray magnetic field.

Axial Stray Magnetic Field Tests

Test results are summarized in **Figure 9**. Insertion loss and isolation of the saturated isolator are shown in the red curves. Insertion loss remains constant at 0.5 dB when subjected to stray axial magnetic fields between 220 Oe and +220 Oe. Isolation drops from 32 dB at – 220 Oe to 25 dB at +220 Oe, indicating that the ferrite rod is slightly too long for peak performance.

Insertion loss and isolation of the traditional isolator are shown in the blue curves. In this case, they vary widely as a function of axial stray magnetic field. With no stray field (H=0), the isolation is 30 dB and insertion loss is 1.7 dB. When the stray axial field is increased by ± 38 Oe, however, both insertion loss and isolation are 4.7 dB; the traditional style isolator degenerates to a bi-directional attenuator. At a magnetic field strength of 80 Oe, isolation and insertion loss values are reversed. The traditional style isolator, once again, behaves as an isolator, but in the reverse direction. The magnetic sheath is clearly ineffective against axial stray magnetic fields. This is not surprising since the sheath has the form of a hollow cylinder with an inner diameter near 25 mm, far from the ferrite rod.

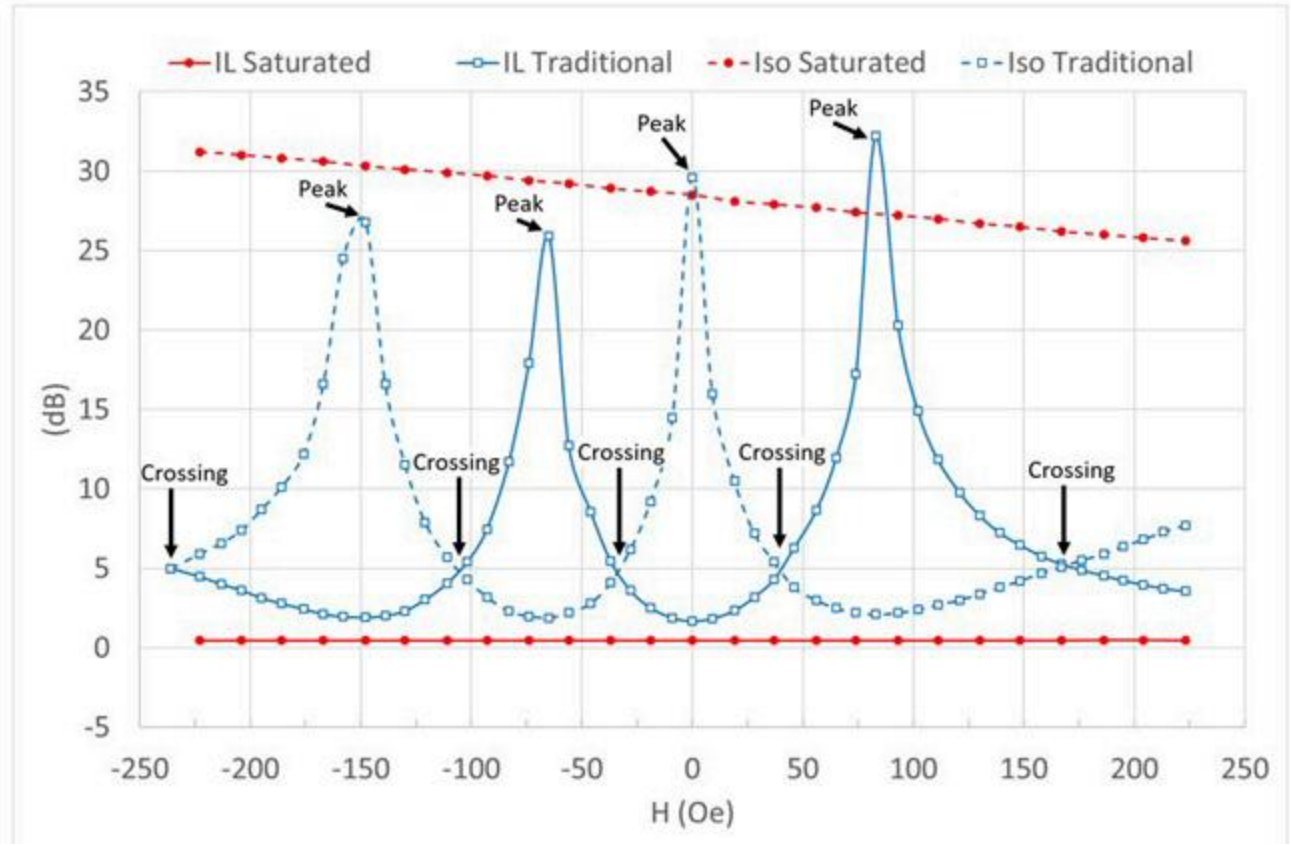

Figure 9 Test data for a saturated (red) and traditional style (blue) isolator under exposure to an axial stray magnetic field. Test data is at taken 92.5 GHz

ANALYSIS

The extrema in the data and the points where isolation and insertion loss curves cross correspond to changes in the signal rotation of N*45 degrees, where N is an integer having the range – 5 to +3 and inclusive of 0. **Figure 10** shows the cross-section of the transition region between the ferrite rod and the rectangular waveguides. The ferrite is indicated by a shaded circle and the orientation of the resistive layer is shown as a dashed line. Since dipole precession is fixed by the magnetic bias field, both the forward and reverse traveling signals rotate in the CCW direction as they pass through the ferrite rod. This is the basis for the non-reciprocal behavior of the Faraday rotation isolator. In the absence of a stray magnetic field, the signals rotate 45 degrees CCW as they make a single pass through the ferrite. The forward traveling signal impinges on the output waveguide with the polarization aligned to the TE_{10} mode and is coupled to the output waveguide. The reverse traveling signal impinges on the input waveguide with the polarization aligned to the resistive layer in the input cone and is absorbed. This is the normal operating condition.

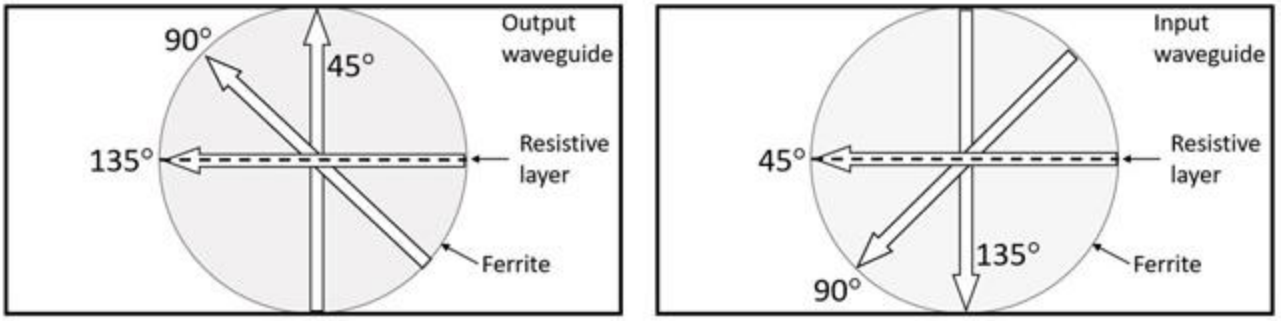

a) Polarization of the forward travelling signal as it exits the ferrite and impinges on the output waveguide.

b) Polarization of the reverse travelling signal as it exits the ferrite and impinges on the input waveguide.

Figure 10 Polarizations of forward (a) and reverse (b) signals after a single pass through the ferrite rod.

If an axial stray magnetic field is applied with sufficient magnitude to double the ferrite magnetization, both the forward and reverse traveling signals undergo an additional 45 degrees of rotation (90 degrees total). The respective signal polarizations are indicated as 90 degrees in Figure 10. Both the forward and reverse traveling signals now have equal vector components aligned to the resistive layer and the TE_{10} mode. Half of the signal power (3 dB) is absorbed in the resistive layer and half couples to the TE_{10} mode. Since the 3 dB split occurs at both the input and output waveguides at exactly the same magnetic bias condition, insertion loss and isolation have the same value ($|S_{21}| = |S_{12}|$). The actual measured values are 4.7 dB rather than 3 dB due to an additional 1.7 dB loss in the ferrite rod.

If the stray magnetic field is further increased so that the rotation increases another 45 degrees (135 degrees total), the reverse traveling signal polarization is aligned to the TE_{10} mode in the input waveguide and the forward traveling signal is aligned to the resistive layer located in the cone in the output waveguide. The signal polarizations are shown labeled as 135 degrees in Figure 10. The isolator now works in the reverse direction, absorbing forward traveling signals and passing reverse traveling signals. Reversing the polarity of the axial stray magnetic field causes the same series of events to occur with the signal rotation now in the clockwise direction.

The measured data in Figure 9 gives the value of the magnetic field, H, for the extrema and the crossings. As described, these are the points at which the rotation is an integer value of 45 degrees. The ferrite rods used in traditional style isolators are typically 6 mm long as reported by Erickson.[9] Using the equation for rotation, Equation (1), with $\theta = 45$ degrees and $l = 6$ mm, yields a magnetization of $4\pi M_Z = 1{,}258$ gauss. Each 45 degree rotation step therefore corresponds to a magnetization increment of 1,258 gauss.

The resulting plots of magnetization, $4\pi M_Z$, versus magnetic field, H, are shown in **Figure 11**. Two curves are shown because of a small hysteresis observed in the data. The red curve is obtained by starting at the highest possible negative field (about – 260 Oe) and reducing the magnitude. The red data points are thus taken in order from left to right on the graph. The blue data points are taken in order from right to left on the graph. The blue and red data points represent the crossings and peaks in the measured data. The dashed lines are fourth order polynomial curve fits to the data.

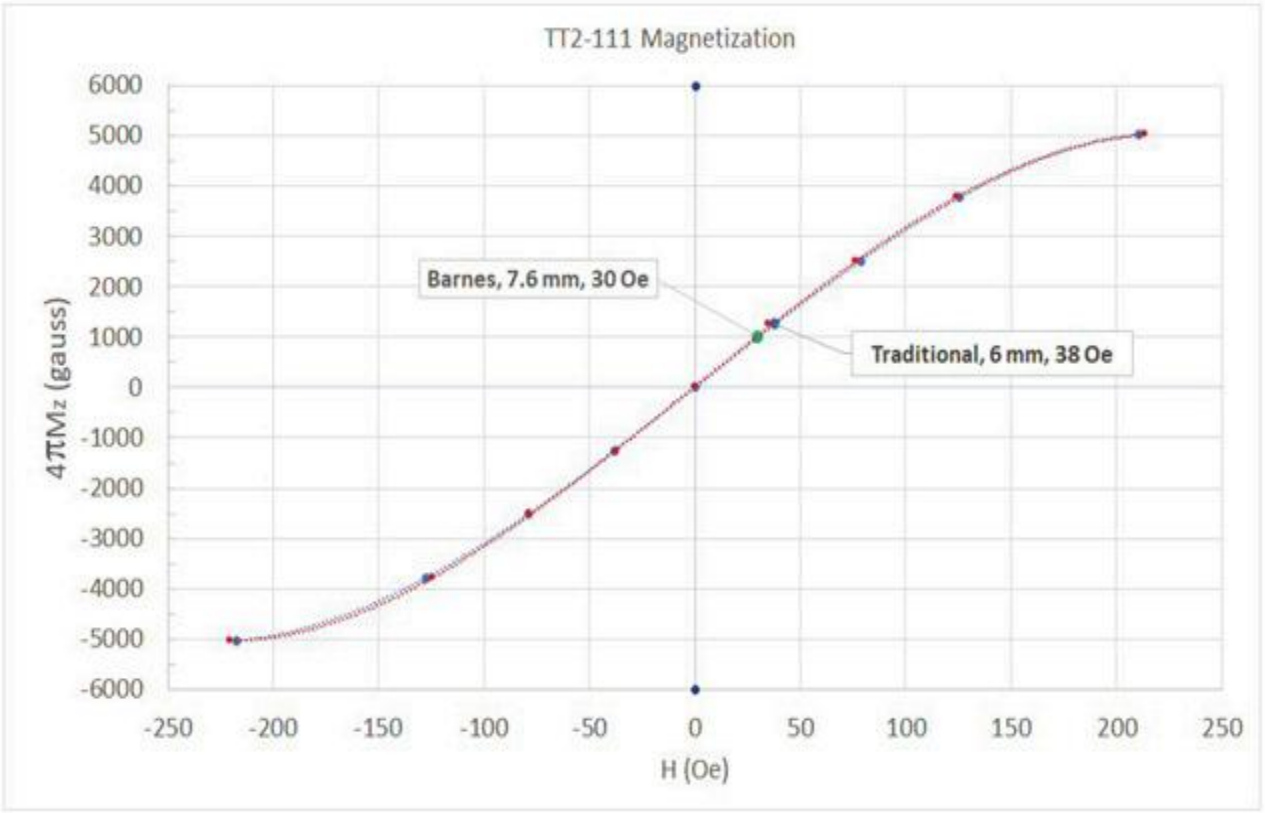

Figure 11 Measured magnetization curves for ferrite with $4\pi M_S$ = 5,000 gauss.[5]

The plotted curves in Figure 11 reach saturation near 5,000 gauss. Negative values of $4\pi M_Z$ are used to denote reversal of the magnetic field polarization. Additional interim data points may be obtained by constructing an isolator with a longer ferrite rod. The magnetic bias point of the traditional style isolator is indicated on the graph. The magnetic bias field used in the Micro Harmonics isolators has been measured at more than 700 Oe and therefore does not fit on the graph. At 700 Oe the bias point is hard into saturation where the slope of the magnetization curve, dM_Z/dH, is near zero, which explains the saturated isolator's insensitivity to stray magnetic fields.

Barnes[4] reported using a 7.6 mm length of ferrite rod with $4\pi M_S$ = 5,000 gauss and a magnetic field near 30 Oe. Using Equation (1), the calculated magnetization required to rotate the signal by 45 degrees is 990 gauss. This data point also falls on the measured magnetization curves in Figure 11.

CONCLUSION

Traditional style Faraday rotation isolators employing a magnetic sheath are highly sensitive to stray magnetic fields. The magnetic sheath gives good protection against stray magnetic fields that are orthogonal to the magnetic bias field but provides little or no protection against axial stray magnetic fields aligned parallel to the bias field. This is expected since the magnetic sheath has the form of a hollow cylinder with an inner diameter near 25 mm, far from the ferrite rod. Figure 11 shows that the magnetic bias point of the traditional isolator is on the steep part of the magnetization curve where small changes in the magnetic bias field, H, give rise to relatively large changes in the magnetization, $4\pi M_Z$. This in turn causes large changes in the signal rotation and results in severely degraded isolator performance. The long ferrite used in traditional style unsaturated isolators also causes high insertion loss at higher millimeter-wave frequencies. The insertion loss of the traditional isolator was measured to be 1.7 dB at 92.5 GHz.

In contrast, magnetically saturated isolators are highly resistant to the effects of stray magnetic fields, both axial and orthogonal, even though the isolators do not employ magnetic sheaths. Resistance to stray magnetic fields arises from the fact that the ferrite is biased hard into saturation where the slope of the magnetization curve is near zero. Relatively large changes in the magnetic bias caused by stray magnetic fields have little effect on the magnetization. Saturated isolators also employ much shorter ferrite rods, which significantly reduces insertion loss. Insertion loss of the Micro Harmonics isolator is 0.5 dB at 92.5 GHz.

ACKNOWLEDGMENTS

We would like to thank NASA JPL for their continued support of this work through research contracts NNX15CP37P, NNX16CP07C, 80NSSC18P2018 and 80NSSC19C0148.

References

1. Q. Z. Ni, E. Daviso, T. V. Can, E. Markhasin, S. K. Jawla, T. M. Swager, R. J. Temkin, J. Herzfeld and R. G. Griffin, “High Frequency Dynamic Nuclear Polarization,” *Accounts of Chemical Research*, Vol. 46, No. 9, April 2013, pp. 1933–1941.
2. M. C. Downer, R. Zgadzaj, A. Debus, U. Schramm and M. C. Kaluza, “Diagnostics for Plasma-Based Electron Accelerators,” *Reviews of Modern Physics*, Vol. 90, August 2018.
3. H. -J. Hartfuß and T. Geist, *Fusion Plasma Diagnostics with mm-Waves: An Introduction*, Wiley-VCH Verlag GmbH & Co, 2013.
4. C.E. Barnes, “Broad-Band Isolators and Variable Attenuators for Millimeter Wavelengths,” *IRE Transactions on Microwave Theory and Techniques*, Vol. 9, No. 6, November 1961, pp. 519-523.
5. “Products for RF/Microwave Applications,” Ferrite TT2-111, *Trans-Tech Corporation*. Web. https://datasheet.octopart.com/SR9000SPQ0472AY-Trans-Tech-datasheet-8861441.pdf.
6. D. Pozar, *Microwave Engineering*, 4th Edition, John Wiley & Sons, 2012.
7. B. Lax and K. Button, *Microwave Ferrites and Ferrimagnetics*, McGraw-Hill, New York, 1962.
8. Constantine A. Balanis, *Advanced Engineering Electromagnetics*, Wiley; 2nd edition, 2012.
9. N. R. Erickson, “Very Low Loss Wideband Isolators for mm-Wavelengths,” *IEEE International Microwave Symposium Digest*, May 2001, pp. 1175-1178.